Rapid Optimization of Photoredox Reactions for Continuous-Flow Systems Using Microscale Batch Technology

María González-Esguevillas, David F. Fernández, Juan A. Rincón, Mario Barberis, Oscar de Frutos, Carlos Mateos, Susana García-Cerrada, Javier Agejas, and David W. C. MacMillan*
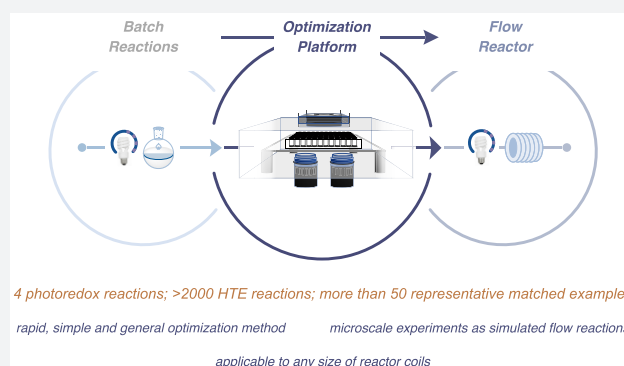
ACCESS | Metrics & More | Article Recommendations | Supporting Information

ABSTRACT: Photoredox catalysis has emerged as a powerful and versatile platform for the synthesis of complex molecules. While photocatalysis is already broadly used in small-scale batch chemistry across the pharmaceutical sector, recent efforts have focused on performing these transformations in process chemistry due to the inherent challenges of batch photocatalysis on scale. However, translating optimized batch conditions to flow setups is challenging, and a general approach that is rapid, convenient, and inexpensive remains largely elusive. Herein, we report the development of a new approach that uses a microscale high-throughput experimentation (HTE) platform to identify optimal reaction conditions that can be directly translated to flow systems. A key design point is to simulate the flow-vessel pathway within a microscale reaction plate, which enables the rapid identification of optimal flow reaction conditions using only a small number of simultaneous experiments. This approach has been validated against a range of widely used photoredox reactions and, importantly, was found to translate accurately to several commercial flow reactors. We expect that the generality and operational efficiency of this new HTE approach to photocatalysis will allow rapid identification of numerous flow protocols for scale.

Batch Reactions — *Optimization Platform* — *Flow Reactor*

4 photoredox reactions; >2000 HTE reactions; more than 50 representative matched examples

rapid, simple and general optimization method — microscale experiments as simulated flow reactions

applicable to any size of reactor coils

■ INTRODUCTION

The past decade has witnessed exponential growth in the development of photoredox catalytic methods for organic synthesis. Photocatalysis, in which photon-harvesting molecules convert light energy to chemical energy, offers many useful advantages. In addition to being ecofriendly and sustainable,[1,2] photocatalytic methods are uniquely capable of promoting challenging bond formations[34] and novel chemical transformations[5−7] due to their ability to access high-energy intermediates in a controlled and selective manner. Photoredox catalysis is now used in the synthesis of agrochemicals, fine chemical intermediates, active pharmaceutical compounds (APIs), and finished dosage forms (FDFs).[8] While photocatalytic methods have found increasing industrial application, one remaining hurdle to widespread adoption of this platform is the inherent complexity in adapting photochemical reactions to large-scale settings, such as those required for process chemistry.[9−13] A critical outcome of the Beer−Lambert Law, with respect to the scale-up of photochemical transformations, is that photon-flux penetration decreases exponentially with depth in a given reaction medium, ultimately leading to attenuation in the transfer of photons.[14] Thus, visible-light-mediated reactions take place only in the proximal area (within 2 mm) of the vessel wall.[15−17] As such, a decrease in the diameter of the reaction vessel should lead to an increase in

photon flux throughout the reaction medium and improved reaction efficiency. This observation has inspired recent efforts to develop (i) laser-based reaction platforms that employ high-intensity photon sources, which in combination with continuous stirred tank reactors (CSTRs) provide powerful improvements with respect to photon penetration in a batch-flow setting, and (ii) continuous-flow photoreactors, which naturally permit better light penetration due to the narrow tubing diameter; such systems have been shown to permit gram- and kilogram-scale transformations.[18,19] In general, flow reactor platforms offer many advantages over batch chemistry[20−26] with respect to photon efficiency, reproducibility, scale-up, safety, waste generation, and productivity regarding both yield and reaction time (Figure 1a). Along these lines, a number of research groups have adopted flow photochemistry strategies for the synthesis of molecules of pharmaceutical interest (Figure 1b).[27−29] Despite these advantages, the optimization of a flow chemistry process typically can be an
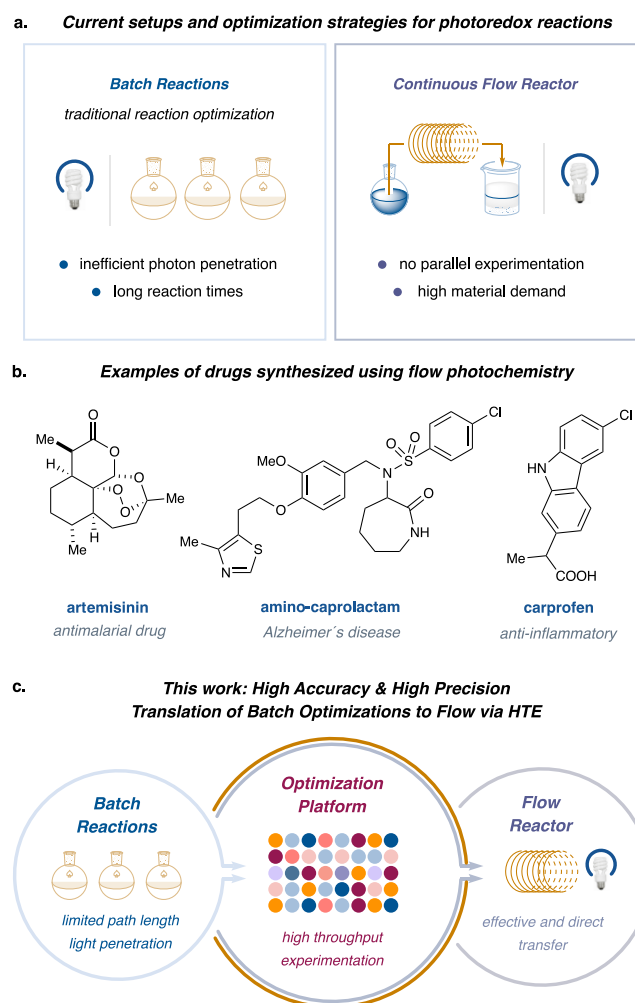
Figure 1. (a) Photoredox reactions can take place in batch, which normally requires a small scale, or in flow, for more efficient light penetration. However, general optimization methods in flow systems remain elusive. (b) Continuous-flow systems have been used for the synthesis of many active pharmaceutical ingredients (ref 28). (c) We disclose a general approach to the optimization of any photoredox reaction from batch to flow using a microscale parallel experimentation to simulate the flow conditions.

onerous task for several reasons: (i) it is traditionally not possible to perform parallel optimization experiments in the context of a flow system; (ii) the optimal reaction conditions are highly dependent on the size of the individual reactor; and (iii) each flow chemistry experiment requires significant amounts of material compared to the analogous reaction conducted in batch.[30,31] A number of strategies have been pursued to streamline optimization of flow-based photoredox methods, including reducing the reaction vessel size,[32−37] leveraging mathematical equations[38] and algorithms,[36,39,40] and adapting new technologies (segmented[41,42] or microflow[43−46] and industry 4.0[47]).

Over the past decade, high-throughput experimentation (HTE) methodologies have been successfully employed in the optimization of numerous catalytic transformations.[48−51] Such technology has been adopted within both academic and industrial settings to allow the evaluation of reaction parameters while minimizing economic and waste constraints. Recently, the optimization of photoredox protocols has also been conducted using HTE technology.[34,35] Using such

strategies, it has been possible to build foundational results from which reaction optimization can be examined thereafter in continuous-flow systems. However, a limitation of existing optimization platforms is the difficulty in translating HTE outcomes to continuous-flow platforms, a feature that often relates to the change in vessel, light intensity, and light path-length considerations.[49,51−55] A complementary approach was beautifully described by the Stephenson group[56] at the outset of the preparation of this manuscript, demonstrating a flow-based HTE platform by developing a droplet microfluidic system for the development of photochemical reactions. This study is focused on the generation of compound libraries, ultimately increasing the chemical space with great time and material efficiency. Notwithstanding, to the best of our knowledge, a general HTE strategy for the translation of optimized photoredox reactions seamlessly to similar outcomes on a flow platform remains undeveloped and would be of a great interest to both discovery programs and process chemistry alike.

With this in mind, we sought to design an HTE platform that mimics the conditions of a flow reactor.[48−55] A requisite goal would be that the optimization data collected via this HTE platform should be directly transferrable to a flow system, permitting the rapid translation of small-scale batch-vessel photoredox reactions to large-scale flow systems. Thus, the HTE setup should allow us to perform miniaturized reactions while simulating continuous photonic flow chemistry protocols.

A compelling benefit of such a system is the ability to simultaneously explore numerous reaction variables, including the catalyst, photon intensity, base, solvent, and so on, in parallel while employing short residence times. We describe herein the development of this HTE platform and its validation in the context of four representative photoredox transformations.

■ FLOSIM PLATFORM DESIGN

Design Plan of an HTE Platform to Simulate Continuous-Flow Systems. Successfully modeling photochemical flow reactions in a high-throughput setting requires designing a system that adequately captures the distribution of photonic energy present throughout the entire protocol employed within the flow apparatus.[57,58]

In a photoredox-catalyzed transformation, wherein the approximations of the Beer−Lambert law operate, the photon absorption is described as a function of the incident radiation and the absorption coefficient.[59] Given the angular and spatial dependence of the spectral specific intensity and the complex geometric considerations required to accurately describe irradiation in flow, we recognized that determining the specific spectral intensity to enable design of a corresponding high-throughput setup would prove to be challenging at best. Importantly, however, we recognized that the key components of spectral intensity could be appropriately accounted for by selection of a light source that results in the same radiant flux for both systems.[60] Furthermore, the incident radiation could now be approximated by ensuring the same path length of irradiation under both flow and high-throughput batch conditions. With this in mid, we sought to accomplish a path-length matching feature by the operationally simple step of varying the volume in a standard 96-well plate to generate a solution height matching the internal diameter (ID) of the transparent fluorinated ethylene propylene (FEP) tubing

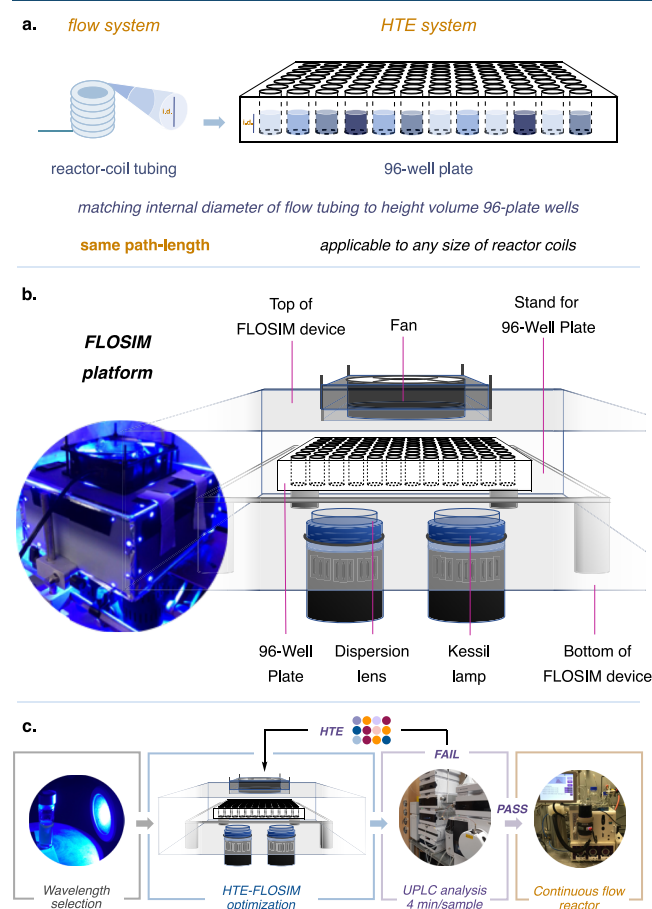chosen of the flow system (Figure 2a, see Supporting Information for details).

Figure 2. Simulation process and sequential optimization method. (a) By using the inner diameter of the reactor-coil tubing as the height on the plate, we can calculate the required reaction volume. (b) To simulate the flow reactor, a reflected FLOSIM device was built and validated across various parameters, such as the position, lights, and cooling system. The FLOSIM device was optimized to obtain both high reactivity in conjunction with homogeneity across the plate. (c) Workflow: Selection of the optimal wavelength for the reaction is followed by optimization in the 96-well glass plate FLOSIM device. After the reaction, the sample is diluted and analyzed by UPLC. The selected conditions are then validated through transfer into the commercial flow system.

Next, in order to simulate the flow-system environment in the context of a photochemical reaction, it would be crucial to recreate the reactor-coil element. Accordingly, we assembled a multienvironment 96-well plate glass device that enables a high level of light exposure (Figure 2b). This platform was equipped with two Kessil LEDs (PR160) and two ThorLabs concave lenses (see Supporting Information for details), while temperature control was maintained through air convection methods. The use of a glass 96-well plate allows complete penetration and reflection of the light inside the device in all directions, and the uniformity of photon dispersion is accomplished across the platform using a ThorLabs concave lens and several high-density reflection mirrors.

In order to evaluate the system's ability to facilitate photoredox reactions with satisfactory consistency within the plate, we conducted a series of simple test reactions using different materials at different positions along the plate (see Supporting Information).[61] In Figure 2c, we outline the general workflow for the translation of a photoredox reaction from batch to flow using a multiscreening platform. Route scouting to identify optimal reaction conditions begins with validation of the reaction, in batch, across different wavelengths. Next, reaction optimization is performed on microscale using the flow simulation (FLOSIM) HTE setup. Briefly, the 96-well glass plate is loaded inside a nitrogen-filled glovebox, sealed with transparent film, and placed in the benchtop HTE device, where it is exposed to light irradiation for a short period of time equivalent to the desired residence time in the flow system. Following completion of screening, the crude reaction mixtures are analyzed by ultraperformance liquid chromatography (UPLC). This two-step process, HTE screening of different conditions, and analysis of results via UPLC, can be performed iteratively until the desired results are obtained.

Last, the optimal conditions, as determined from the HTE microscale platform, were directly reproduced in the commercial flow system using the preferred wavelength, light intensity, substrate/reagent concentrations, residence time, solvent, base, and so on. As described below, the optimized conditions identified at the 60 μL scale in the glass plate system were found to be directly transferrable to a UV-150 Vapourtec E-Series system equipped with a 2 mL or 10 mL reactor coil. We have demonstrated the utility and generality of this FLOSIM HTE optimization protocol in the context of four representative photocatalytic reactions widely employed in medicinal chemistry.

■ RESULTS AND DISCUSSION

Optimization of Decarboxylative Arylation for Flow. In 2014, we reported a novel decarboxylative arylation,[62] wherein amino acids are transformed into benzylic amines under synergistic photoredox and nickel catalysis (Figure 3a). In optimizing this transformation for a flow system, we selected N-Boc-Proline (Boc-Pro-OH) and 1-bromo-4-(trifluoromethyl)-benzene as model substrates. We first validated the reaction using a bench setup: under published conditions with a 26 W CFL light bulb and Cs_2CO_3 base, the desired product was isolated in 88% yield after 36 h. We began optimization studies by evaluating the efficiency of the decarboxylative arylation across a variety of wavelengths (PR160 Kessil LEDs); these investigations revealed 427 nm to be the optimal wavelength for the transformation. An important consideration in developing flow reactions is the need to avoid heterogeneous conditions,[63−65] which often clog the tubular flow reactors. With this criterion in mind, we set out to optimize the transformation using the HTE FLOSIM−UPLC setup, with an eye toward identifying suitable organic bases and solvents to ensure a homogeneous solution (see Supporting Information). Approximately 300 "flow-type" reaction conditions were tested in short order to examine the effect of residence time, solvent, concentration, organic base, photocatalyst, catalyst loading, as well as the nature of the transition metal complex (see Supporting Information). As shown in Figure 3b, these studies led to the identification of homogeneous conditions that afforded the desired transformation in only 45 min with 79% yield. We next sought to transfer these conditions to a flow platform: a UV-150 Vapourtec E-Series system equipped with a 2 mL reactor coil and 420 nm LED. We were pleased to find that the HTE-optimized reaction conditions were directly
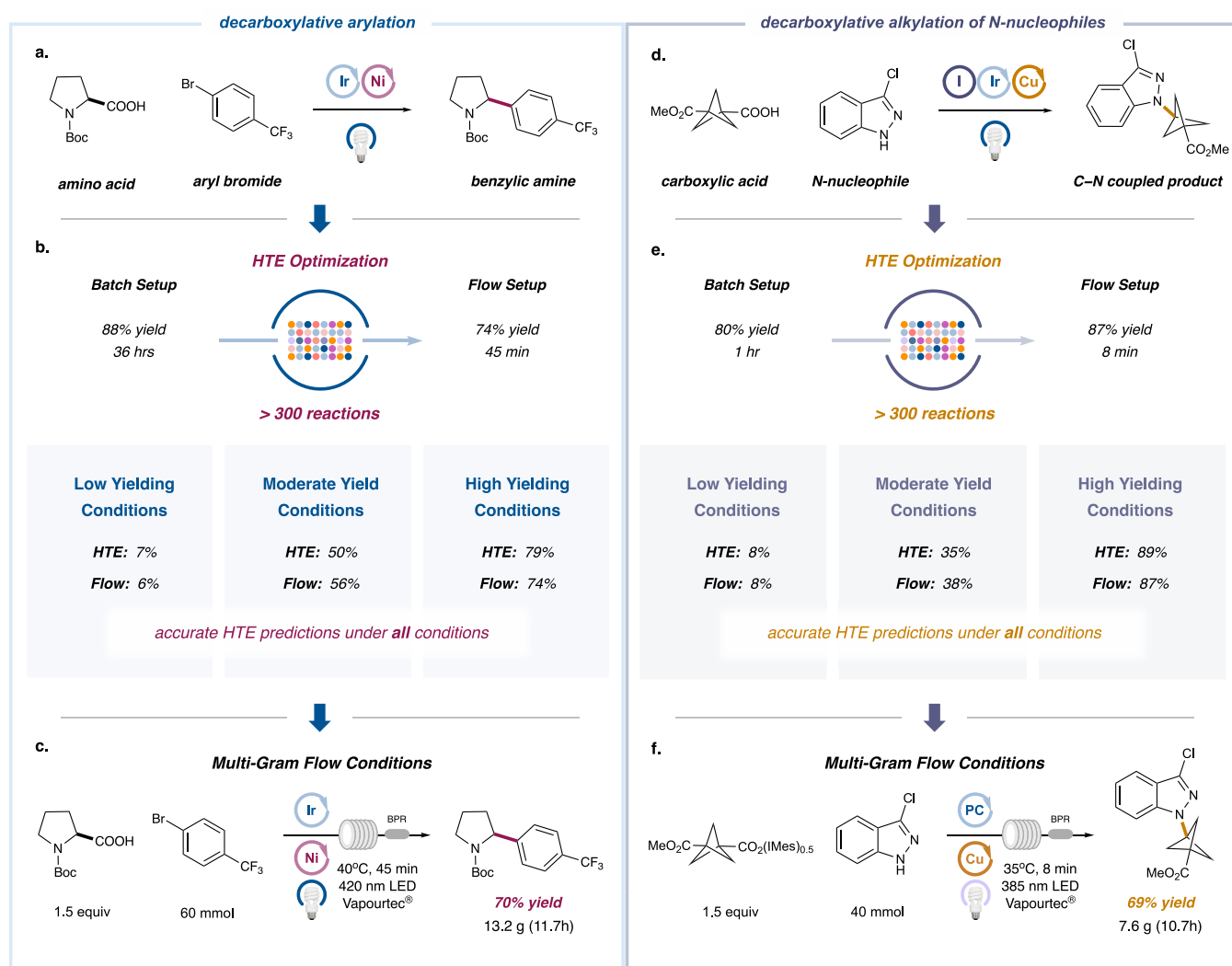
Figure 3. C−C and C−N coupling via decarboxylative protocols. (a) The reaction between N-Boc-proline with 1-bromo-4-(trifluoromethyl)-benzene was evaluated with a variety of light sources using standard conditions; superior results were obtained with the 427 nm LEDs (see Supporting Information). (b) A range of results have been obtained for several conditions, with high, moderate, or low yield being replicated between the FLOSIM device and the commercial flow setup (see Supporting Information). (c) The reaction was successfully scaled using a Vapourtec E-Series with a 10 mL reactor coil (1.3 mm ID). (d) Reaction between activated carboxylic acid iodonium salts and 3-chloro-indazole as the N-nucleophile via dual-photoredox copper catalysis. Superior results were obtained with a 390 nm Kessil LED light source. (e) A range of results have been obtained for several conditions, with high, moderate, or low yield being replicated between the FLOSIM device and the commercial flow setup (see Supporting Information). (f) The reaction was successfully scaled at a 40 mmol level affording 7.6 g of the desired product (69% yield) using a Vapourtec E-Series with a 10 mL reactor coil (1.3 mm ID). PC corresponds to 4CzIPN.

translatable to the Vapourtec, delivering the desired product with comparable levels of efficiency (74% yield) using the same conditions including 45 min of residence time (Figure 3b). In order to be confident that the HTE platform offers an accurate simulation of the Vapourtec flow system, we sought to determine the consistency of data between both systems using a variety of reaction conditions. As shown in Figure 3b, we selected two sets of conditions that gave mediocre and poor results respectively with the HTE setup (i.e., 50 and 7% yield). Indeed, when these suboptimal conditions were transferred to the Vapourtec reactor, we again found a remarkable level of consistency between the HTE FLOSIM batch reactors and the flow efficiencies (56 and 6% yield, respectively). These results suggest that the optimization data obtained in the context of the HTE platform are, indeed, indicative of performance in flow. Moreover, time studies conducted for both the HTE setup and the flow setup under optimal conditions reveal a

strong correlation between the two systems with respect to conversion as a function of reaction time (see Supporting Information).

Next, we aimed to demonstrate the feasibility of this flow-optimized method in processes of different scale. As shown in Figure 3c, when the reaction was conducted at the 60 mmol level using the optimized conditions with a larger coil size reactor (10 mL), the desired product was isolated in 70% yield. Moreover, 13.2 g of product was isolated after an 11.7 h total flow reactor time using the Vapourtec system. In comparison to the laboratory vial reactor procedure, which provides 111 mg of desired product in 36 h, we were able to demonstrate a 366-fold increase in efficiency by way of this rapid, flow optimization protocol.

Optimization of C−N Arylation Coupling for Flow. In 2018, our group reported a new transformation that allows the decarboxylative alkylation of N-nucleophiles via the merger of
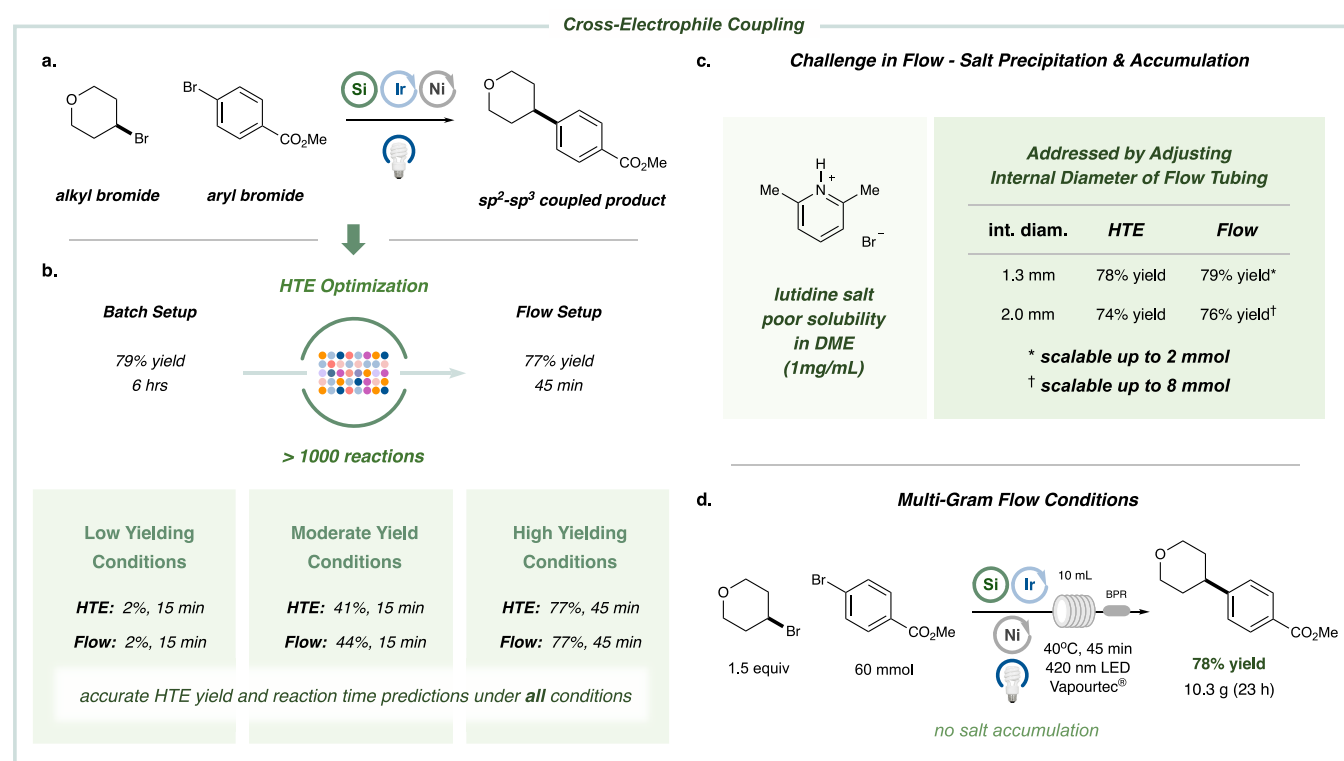
Figure 4. Optimization platform for cross-electrophile coupling. (a) The reaction takes place between 4-bromotetrahydropyrane and methyl-4-bromobenzoate via silane-mediated metallaphotoredox catalysis using 427 nm Kessil LEDs as the optimal light source (see Supporting Information). (b) HTE optimization allows the desired product in the flow system (77% yield) to be obtained in 45 min of residence time instead 6 h of reaction time using a standard setup. Several conditions were evaluated for both setups (see Supporting Information for exact experimental conditions). (c) Lutidinium bromide was detected during the course of the reaction obstructing the flow reactor coil by accumulation. The use of thicker tubing allows the reaction to be scaled up to 8 mmol. (d) The effectivity of this reaction has been proved using a 60 mmol scale affording 10.3 g of the desired product (78% yield).

photoredox and copper catalysis.[66] Among a large scope of valuable alkylation substrates, there has been growing interest in the incorporation of rigid bicyclic structures, such as [1.1.1]-propellane (BCP) scaffolds, into medicinal compounds, owing to their capacity to act as bioisosteres of alkynes or para-substituted benzene rings. With this consideration in mind, we sought to optimize a flow method for the rapid production of molecules containing the BCP scaffold via our C−N coupling platform. We selected 3-(methoxycarbonyl)bicyclo[1.1.1]-pentane-1-carboxylic acid and 3-chloro-indazole as the model coupling partners. Using our previously published conditions, the C−N coupling adduct was obtained in a vial batch in 80% yield after 1 h. After a subsequent survey of reaction efficiencies as a function of LED wavelength, it became apparent that the coupling proceeds well across a variety of light sources, and 390 nm was selected for further HTE studies (see Supporting Information). As shown in Figure 3e, following a short HTE FLOSIM−UPLC optimization campaign that involved the assessment of ~300 reactions (evaluating different reaction times, solvents, concentrations, catalysts and catalyst loadings, see Supporting Information), we identified optimal flow conditions that provided comparable efficiency (89% yield) within only an 8 min reaction time.

These conditions were then directly transferred to the continuous-flow system (Vapourtec E-Series, 2 mL reactor coil), and a similar result was obtained (87% yield, 8 min residence time). As shown in Figure 3e, a time study showed comparable levels of conversion between the HTE and

commercial flow setups for a variety of conditions that were examined, lending further support to the predictive power of the HTE setup (Figure 3e).

Finally, the decarboxylative alkylation was performed on a 40 mmol scale using our optimized FLOSIM conditions on a Vapourtec reactor (385 nm LEDs, 10 mL reactor coil). The reaction was conducted in the heated mode at 35 °C to prevent solvent freezing. Under the conditions shown in Figure 3f, 7.6 g of the desired product was isolated in good yield (69%) after only 10 h, representing a 6.5-fold increase in reaction efficiency over the vial batch setup.

Optimization of Cross-Electrophile Coupling for Flow. In 2016, we developed a cross-electrophile coupling that has found broad application across a variety of medicinal chemistry campaigns.[67] As such, the development of a simple protocol by which to translate small-scale cross-electrophile couplings to commercial flow systems would have significant benefit for the scale-up of critical building blocks and drug-like fragments or products. Under our standard vial batch setup, the model substrates, 4-bromotetrahydropyran and methyl-4-bromobenzoate, underwent cross-coupling to afford the desired product in 79% yield over the course of 6 h. Moreover, irradiation at 427 nm was observed to be optimal for this transformation (see Supporting Information). Given that HBr is generated as the main byproduct in this coupling protocol,[17] we undertook an evaluation of various soluble organic bases. While initial FLOSIM studies revealed that 2,6-lutidine appeared to be an effective acid scavenger and compatible with high coupling yields, the resulting side product, a
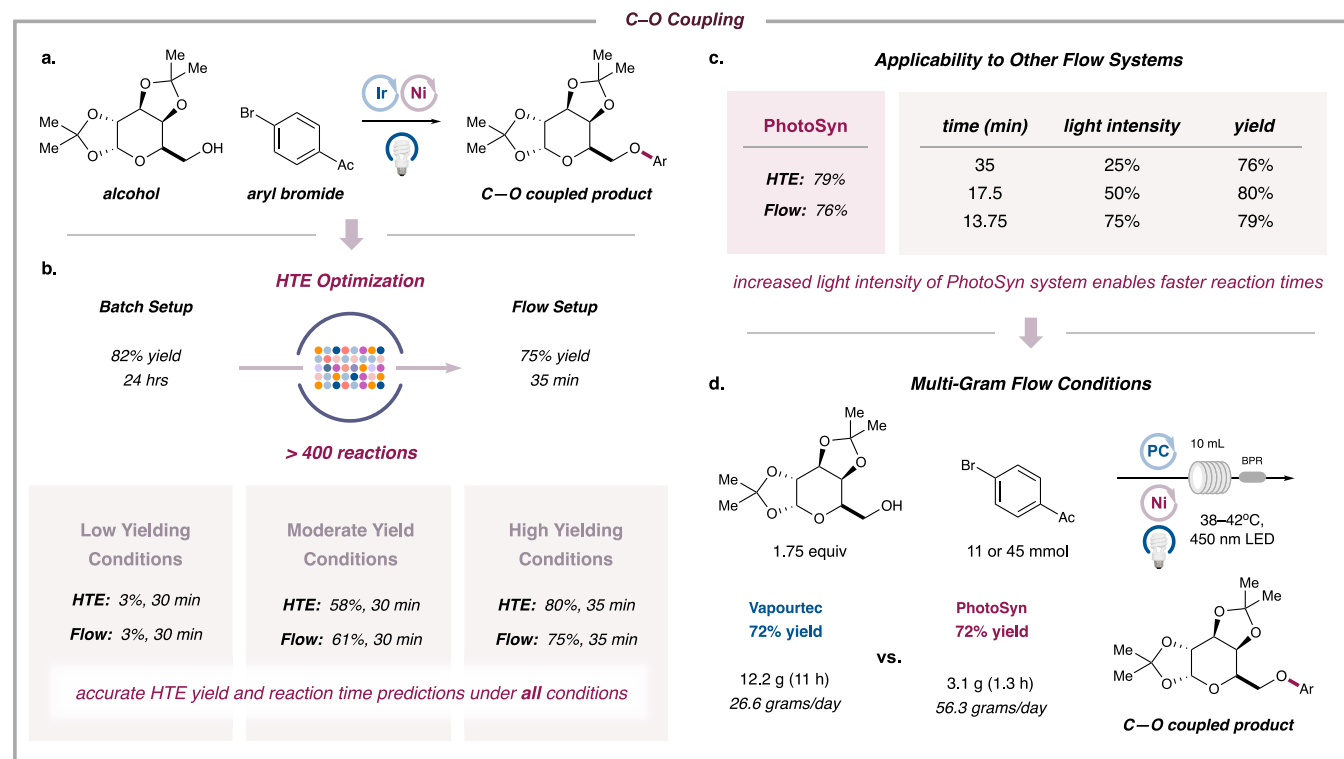
Figure 5. Application for C−O coupling reaction. (a) The reaction takes place between protected pyranose and 4-bromo-acetophenone merging nickel and photoredox catalysis. (b) With the workflow shown using 456 nm Kessil LEDs, followed by HTE optimization and the corresponding UPLC analysis, we could obtain in a flow system the desired product (75% yield) in 35 min of residence time instead 24 h of reaction time using a standard setup. Optimization using our HTE protocol provides a range of conditions, which we could translate successfully to the flow system. (c) The efficiency of our protocol was also proved by using a powerful continuous-flow system (PhotoSyn). Using the 25% light intensity, we could observe a correlated result with our HTE setup. Furthermore, increasing the light intensity, we were able to reduce the reaction time with no changes on the reactivity. (d) The effectivity of this reaction has been proved for both continuous-flow systems affording the same reactivity (72% yield), resulting in a higher efficiency for the more powerful flow system (26.6 g/day for Vapourtec and 56.3 g/day using PhotoSyn.

lutidinium bromide salt, has poor solubility and ultimately causes the flow system to clog. As such, we were unable to translate this initial set of HTE-optimized conditions beyond an 8 mmol scale using the commercial flow reactor (Figure 4c; also see Supporting Information) due to the need to incorporate frequent wash cycles to remove salt byproducts.

Given the broad interest in this coupling protocol across the industrial sector,[68−70] we undertook a second optimization campaign using the HTE FLOSIM device, with the goal of identifying homogeneous conditions that would provide improved properties for scale-up. In this regard, we performed approximately 1000 experiments via HTE FLOSIM to evaluate a variety of reaction components (bases, solvents, concentrations, reaction times, metal complexes, catalyst loadings, additives, and cosolvents; see Supporting Information). Through this process, we determined that (i) decreasing the amount of base from 2 to 1 equiv, (ii) switching to a more polar solvent [N,N-dimethylacetamide (DMA)], and (iii) extending the reaction time to 45 min provided optimal efficiency without issues related to salt precipitates. Moreover, with these conditions in hand, we were able to achieve high efficiency in both the HTE setup (77% yield) and the commercial flow system (77% yield) (Figure 4d). Most importantly, as shown in Figure 4d, we were able to scale this reaction to 60 mmol using the Vapourtec E-Series (10 mL reactor coil and 420 nm LEDs) to obtain 10.3 g of the coupled product in 78% yield after 23 h.

In comparison to the initial vial batch protocol (87 mg obtained), this result represents a 30.9-fold improvement in efficiency.

Optimization of Visible-Light-Mediated C−O Arylation Coupling for Flow. Our photocatalytic C−O coupling reaction[71] has emerged as a versatile strategy for the synthesis of alkyl aryl ethers. Under the standard bench setup, using a relatively complex protected pyranose model substrate and an aryl bromide, the etherification generated the desired product in 82% yield after 24 h. Irradiation at 456 nm was found to provide optimal reaction efficiency (see Supporting Information). Optimization studies with the HTE FLOSIM platform (~450 experiments to evaluate all the components in the reaction, see Supporting Information) revealed the inexpensive organic photocatalyst, 2,4,5,6-tetra(9H-carbazol-9-yl)-isophthalonitrile (4CzIPN), to be the ideal catalyst, generating the coupling product in 80% yield after 35 min (Figure 5b). Translating these optimal HTE conditions to the commercial flow system yielded similar results (75% yield), and time studies demonstrated a strong correlation between these two platforms. Once again, the results generated from the HTE system were consistent with those obtained from the flow system across a variety of optimal and nonoptimal conditions (Figure 5b).

Translation of the HTE FLOSIM Platform to Multiple Commercial Flow Reactors. Throughout most of this project, we employed a UV-150 Vapourtec E-Series as a representative flow reactor for scale-up. In order to

demonstrate the generality of this approach for practitioners in this field, we sought to test our protocol in a second, commercial flow system. In this context, we evaluated the PhotoSyn flow photoreactor as developed and manufactured by Uniqsis Ltd. This photoreactor is equipped with a 10 mL reactor coil (ID = 1.0 mm) and more powerful LEDs (455 nm LEDs, 700 W total power, approximately 200 W output power) compared to the Vapourtec system. According to literature precedent,[33] flow reactors that incorporate high-powered photonic sources may offer numerous benefits, including faster reaction rates, shorter reaction times, and amenability to nonhomogeneous conditions. On this basis, we evaluated the efficiency of the above-mentioned C−O coupling protocol in the PhotoSyn flow system using various light intensities as determined via our HTE FLOSIM platform. As shown in Figure 5c, using 25% light intensity, we were able to achieve satisfactory yield (76% yield in HTE FLOSIM vs 79% in PhotoSyn) with a residence time of 35 min. Moreover, by increasing the light intensity to 75%, we obtained a comparable 79% yield with a much shorter reaction time of 13.75 min (Figure 5c, also see Supporting Information). Finally, we attempted a gram-scale synthesis of the product with each continuous-flow system (Figure 5d). Under optimized conditions, the Vapourtec system provided 12.2 g of final product in 11 h (72% yield), while the PhotoSyn system is able to generate 26.2 g of the same product in the same time frame (72% yield). Thus, compared to a batch setup, which provides 310 mg of product in 24 h, the flow system can lead to an 86-fold efficiency acceleration using the Vapourtec system and 185-fold efficiency enhancement using the PhotoSyn photoreactor. More importantly, we have demonstrated that our HTE FLOSIM optimization strategy can be applied across various commercial flow reactors.

CONCLUSION

In summary, we have designed an HTE FLOSIM device that can simulate a continuous-flow setup to enable the optimization and direct translation of small-scale photoredox methods to large-scale flow reactors. This system permits the reproduction of the same reaction pathways in both an HTE setup and a continuous-flow setup and therefore serves as a general platform to rapidly optimize any photoredox reaction at microscale. We have evaluated this optimization platform in the context of four prominent photocatalytic transformations, and in each case, we have been able to significantly improve the efficiency of these methodologies at large scale compared to standard batch conditions. Moreover, the generality of this platform with regard to different flow reactors has been demonstrated. Considering the widespread interest in photoredox catalysis across the pharmaceutical industry, we expect this optimization platform to be widely adopted in both medicinal and process chemistry settings.

ASSOCIATED CONTENT

Ⓢ Supporting Information

The Supporting Information is available free of charge at https://pubs.acs.org/doi/10.1021/acscentsci.1c00303.

Experimental procedures and spectral data (PDF)

AUTHOR INFORMATION

Corresponding Author

David W. C. MacMillan − *Merck Center for Catalysis at Princeton University, Princeton, New Jersey 08544, United States;* ⓘ orcid.org/0000-0001-6447-0587; Email: dmacmill@princeton.edu

Authors

María González-Esguevillas − *Merck Center for Catalysis at Princeton University, Princeton, New Jersey 08544, United States;* ⓘ orcid.org/0000-0003-3779-5516

David F. Fernández − *Merck Center for Catalysis at Princeton University, Princeton, New Jersey 08544, United States;* ⓘ orcid.org/0000-0003-3482-0894

Juan A. Rincón − *Centro de Investigación Eli Lilly, S. A., 28108 Madrid, Spain*

Mario Barberis − *Centro de Investigación Eli Lilly, S. A., 28108 Madrid, Spain*

Oscar de Frutos − *Centro de Investigación Eli Lilly, S. A., 28108 Madrid, Spain*

Carlos Mateos − *Centro de Investigación Eli Lilly, S. A., 28108 Madrid, Spain*

Susana García-Cerrada − *Centro de Investigación Eli Lilly, S. A., 28108 Madrid, Spain*

Javier Agejas − *Centro de Investigación Eli Lilly, S. A., 28108 Madrid, Spain*

Complete contact information is available at:
https://pubs.acs.org/10.1021/acscentsci.1c00303

Author Contributions

M.G.-E. and D.F.F. performed and analyzed the experiments. M.G.-E, D.F.F., and D.W.C.M. designed the experiments. J.A.R., M.B., O.F., C.M., S.G.-C., and J.A. provided intellectual contributions. M.G.-E, D.F.F., and D.W.C.M. prepared this manuscript.

Notes

The authors declare no competing financial interest.

ACKNOWLEDGMENTS

REFERENCES

(1) Protti, S.; Dondi, D.; Fagnoni, M.; Albini, A. Assessing photochemistry as a Green synthetic method. Carbon−carbon bond forming reactions. *Green Chem.* **2009**, *11*, 239−249.

(2) Huo, H.; Shen, X.; Wang, C.; Zhang, L.; Röse, P.; Chen, L.-A.; Harms, K.; Marsch, M.; Hilt, G.; Meggers, E. Asymmetric photoredox transition-metal catalysis activated by visible light. *Nature* **2014**, *515*, 100−103.

(3) Shaw, M. H.; Twilton, J.; MacMillan, D. W. C. Photoredox Catalysis in Organic Chemistry. *J. Org. Chem.* **2016**, *81*, 6898−6926.

(4) Twilton, J.; Le, C.; Zhang, P.; Shaw, M. H.; Evans, R. W.; MacMillan, D. W. C. The Merger of Transition Metal and Photocatalysis. *Nat. Rev. Chem.* **2017**, *1*, 0052.

(5) Romero, N. A.; Nicewicz, D. A. Organic Photoredox Catalysis. *Chem. Rev.* **2016**, *116*, 10075−10166.

(6) Staveness, D.; Bosque, I.; Stephenson, C. R. J. Free Radical Chemistry Enabled by Bisible Light-Induced Electron Transfer. *Acc. Chem. Res.* **2016**, *49*, 2295−2306.

(7) McAtee, R. C.; McClain, E. J.; Stephenson, C. R. J. Illuminating Photoredox Catalysis. *Trends Chem.* **2019**, *1*, 111−125.

(8) Prier, C. K.; Rankic, D. A.; MacMillan, D. W. C. Visible Light Photoredox Catalysis with Transition Metal Complexes: Applications in Organic Synthesis. *Chem. Rev.* **2013**, *113*, 5322−5363.

(9) Darvas, F.; Dormán, G.; Hessel, V., Eds. *Flow Chemistry, Vol. 2: Applications*; De Gruyter, 2014.

(10) Beeler, A. B.; Corning, S. R. Photochemistry in flow. *Photochemistry* **2015**, *43*, 173−190.

(11) Vaccaro, L., Ed. *Sustainable Flow Chemistry: Methods and Applications*; John Wiley & Sons, 2017.

(12) Luis, S. V.; García-Verdugo, E., Eds. *Flow Chemistry: Integrated Approaches for Practical Applications*; RSC Publishing, 2019.

(13) May, S. A. Flow Chemistry, Continuous Processing, and Continuous Manufacturing: A Pharmaceutical Perspective. *J. Flow Chem.* **2017**, *7*, 137−145.

(14) Gilmore, K.; Seeberger, P. H. Continuous Flow Photochemistry. *Chem. Rec.* **2014**, *14*, 410−418.

(15) Shvydkiv, O.; Gallagher, S.; Nolan, K.; Oelgemöller, M. From Conventional to Microphotochemistry: Photodecarboxylation Reactions Involving Phthalimides. *Org. Lett.* **2010**, *12*, 5170−5173.

(16) Cambié, D.; Bottecchia, C.; Straathof, N. J. W.; Hessel, V.; Noël, T. Applications of Continuous-Flow Photochemistry in Organic Synthesis, Material Science, and Water Treatment. *Chem. Rev.* **2016**, *116*, 10276−10341.

(17) Photoredox-catalyzed reactions are typically performed at small scales (0.1 to 1.0 mmol) in small reaction vessels (4−10 mm in diameter) and require prolonged reaction times. Our group, in collaboration with Merck, recently produced an integrated photo-reactor system, constructed with a modular design, that provides standardization and acceleration of photocatalytic reactions with better reproducibility at small scale: Le, C.; Wismer, M. K.; Shi, Z.-C.; Zhang, R.; Conway, D. V.; Li, G.; Vachal, P.; Davies, I. W.; MacMillan, D. W. C. A General Small-Scale Reactor To Enable Standardization and Acceleration of Photocatalytic Reactions. *ACS Cent. Sci.* **2017**, *3*, 647−653.

(18) Chen, Y.; de Frutos, O.; Mateos, C.; Rincon, J. A.; Cantillo, D.; Kappe, C. O. Continuous Flow Photochemical Benzylic Bromination of a Key Intermediate in the Synthesis of a 2-Oxazolidinone. *ChemPhotoChem.* **2018**, *2*, 906−912.

(19) Rehm, T. H. Reactor technology concepts for flow photochemistry. *ChemPhotoChem.* **2020**, *4*, 235−254.

(20) Tucker, J. W.; Zhang, Y.; Jamison, T. F.; Stephenson, C. R. J. Visible-Light Photoredox Catalysis in Flow. *Angew. Chem., Int. Ed.* **2012**, *51*, 4144−4147.

(21) Nguyen, J. D.; Reiß, B.; Dai, C.; Stephenson, C. R. J. Batch to flow deoxygenation using visible light photoredox catalysis. *Chem. Commun.* **2013**, *49*, 4352−4354.

(22) Garlets, Z. J.; Nguyen, J. D.; Stephenson, C. R. J. *Isr. J. Chem.* **2014**, *54*, 351−360.

(23) Elliott, L. D.; Knowles, J. P.; Koovits, P. J.; Maskill, K. G.; Ralph, M. J.; Lejeune, G.; Edwards, L. J.; Robinson, R. I.; Clemens, I. R.; Cox, B.; et al. Batch versus Flow Photochemistry: A Revealing Comparison of Yield and Productivity. *Chem. - Eur. J.* **2014**, *20*, 15226−15232.

(24) Noël, T. A personal Perspective on the Future of Flow Photochemistry. *J. Flow Chem.* **2017**, *7*, 87−93.

(25) Plutschack, M. B.; Pieber, B.; Gilmore, K.; Seeberger, P. H. The Hitchhiker's Guide to Flow Chemistry. *Chem. Rev.* **2017**, *117*, 11796−11893.

(26) Wong, J. Y. F.; Tobin, J. M.; Vilela, F.; Barker, G. Batch versus Flow Lithiation-Substitution of 1,3,4-Oxadiazoles: Exploitation of Unstable Intermediates Using Flow Chemistry. *Chem. - Eur. J.* **2019**, *25*, 12439−12445.

(27) Porta, R.; Benaglia, M.; Puglisi, A. Flow Chemistry: Recent Developments in the Synthesis of Pharmaceutical Products. *Org. Process Res. Dev.* **2016**, *20*, 2−25.

(28) Politano, F.; Oksdath-Mansilla, G. Light on the Horizon: Current Research and Future Perspectives in Flow Photochemistry. *Org. Process Res. Dev.* **2018**, *22*, 1045−1062.

(29) Ruffoni, A.; Juliá, F.; Svejstrup, T. D.; McMillan, A. J.; Douglas, J. J.; Leonori, D. Practical and regioselective amination of arenes using alkyl amines. *Nat. Chem.* **2019**, *11*, 426−433.

(30) Abdiaj, I.; Alcázar, J. Improving the throughput of batch photochemical reactions using flow: Dual photoredox and nickel catalysis in flow for C(sp2)−C(sp3) cross-coupling. *Bioorg. Med. Chem.* **2017**, *25*, 6190−6196.

(31) Poscharny, K.; Fabry, D. C.; Heddrich, S.; Sugiono, E.; Liauw, M. A.; Rueping, M. Machine assisted reaction optimization: A self-optimizing reactor system for continuous-flow photochemical reactions. *Tetrahedron* **2018**, *74*, 3171−3175.

(32) Examples using small reaction vessels such as NMR tubes for flow optimization, see: Andrews, R. S.; Becker, J. J.; Gagné, M. R. A. Photoflow Reactor for the Continuous Photoredox-Mediated Synthesis of C-Glycoamino Acids and C-Glycolipids. *Angew. Chem., Int. Ed.* **2012**, *51*, 4140−4143. See also ref 33.

(33) Lima, F.; Grunenberg, L.; Rahman, H. B. A.; Labes, R.; Sedelmeier, J.; Ley, S. V. Organic photocatalysis for the radical couplings of boronic acid derivatives in batch and flow. *Chem. Commun.* **2018**, *54*, 5606−5609.

(34) Reports using high-throughput screening: Vilé, G.; Richard-Bildstein, S.; Lhuillery, A.; Rueedi, G. Electrophile, Substrate Functionality, and Catalyst Effects in the Synthesis of α-Mono and Di-Substituted Benzylamines via Visible-Light Photoredox Catalysis in Flow. *ChemCatChem* **2018**, *10*, 3786−3794. See also refs 35 and 36.

(35) Grainger, R.; Heightman, T. D.; Ley, S. V.; Lima, F.; Johnson, C. N. Enabling synthesis in fragment-based drug discovery by reactivity mapping: photoredox-mediated cross-dehydrogenative heteroarylation of cyclic amines. *Chem. Sci.* **2019**, *10*, 2264−2271.

(36) Kashani, S. K.; Jessiman, J. E.; Newman, S. G. Exploring Homogeneous Conditions for Mild Buchwald-Hartwing Amination in Batch and Flow. *Org. Process Res. Dev.* **2020**, *24* (10), 1948−1954.

(37) For a nonphotonic approach using HTE technologies, see: Perera, D.; Tucker, J. W.; Brahmbhatt, S.; Helal, C. J.; Chong, A.; Farrell, W.; Richardson, P.; Sach, N. W. A platform for automated nanomole-scale reaction screening and micromole-scale synthesis in flow. *Science* **2018**, *359*, 429−434.

(38) Elliott, L. D.; Knowles, J. P.; Stacey, C. S.; Klauber, D. J.; Booker-Milburn, K. I. (2018) Using batch reactor results to calculate optimal flow rates for the scale-up of UV photochemical reactions. *React. Chem. Eng.* **2018**, *3*, 86−93.

(39) Gromski, P. S.; Henson, A. B.; Granda, J. M.; Cronin, L. How to explore chemical space using algorithms and automation. *Nat. Rev.* **2019**, *3*, 119−128.

(40) Baumgartner, L. M.; Dennis, J. M.; White, N. A.; Buchwald, S. L.; Jensen, K. F. Use of a Droplet Platform To Optimize Pd-Catalyzed C−N Coupling Reactions Promoted by Organic Bases. *Org. Process Res. Dev.* **2019**, *23*, 1594−1601.

(41) Hsieh, H.-W.; Coley, C. W.; Baumgartner, L. M.; Jensen, K. F.; Robinson, R. I. Photoredox Iridium−Nickel Dual-Catalyzed Decarboxylative Arylation Cross-Coupling: From Batch to Continuous Flow via Self-Optimizing Segmented Flow Reactor. *Org. Process Res. Dev.* **2018**, *22*, 542−550.

(42) For a nonphotonic version, see: Hwang, Y.-J.; Coley, C. W.; Abolhasani, M.; Marzinzik, A. L.; Koch, G.; Spanka, C.; Lehmann, H.; Jensen, K. F. Segmented Flow Platform for On-Demand Medicinal Chemistry and Compound Synthesis in Oscillating Droplets. *Chem. Commun.* **2017**, *53*, 6649−6652.

(43) McMullen, J. P.; Stone, M. T.; Buchwald, S. L.; Jensen, K. F. An Integrated Microreactor System for Self-Optimization of a Heck Reaction: From Micro- to Mesoscale Flow Systems. *Angew. Chem., Int. Ed.* **2010**, *49*, 7076−7080.

(44) Oelgemöller, M.; Shvydkiv, O. Recent Advances in Microflow Photochemistry. *Molecules* **2011**, *16*, 7522−7550.

(45) Bédard, A.-C.; Adamo, A.; Aroh, K. C.; Russell, M. G.; Bedermann, A. A.; Torosian, J.; Yue, B.; Jensen, K. F.; Jamison, T. F. Reconfigurable system for automated optimization of diverse chemical reactions. *Science* **2018**, *361*, 1220−1225.

(46) Chatterjee, S.; Guidi, M.; Seeberger, P. H.; Gilmore, K. Automated radial synthesis of organic molecules. *Nature* **2020**, *579*, 379−384.

(47) Mateos, C.; Nieves-Remacha, M. J.; Rincón, J. A. (2019) Automated platforms for reaction self-optimization in flow. *React. Chem. Eng.* **2019**, *4*, 1536−1544.

(48) Sun, S.; Kennedy, R. T. Droplet Electrospray Ionization Mass Spectrometry for High Throughput Screening for Enzyme Inhibitors. *Anal. Chem.* **2014**, *86*, 9309−9314.

(49) Buitrago Santanilla, A.; Regalado, E. L.; Pereira, T.; Shevlin, M.; Bateman, K.; Campeau, L.-C.; Schneeweis, J.; Berritt, S.; Shi, Z.-C.; Nantermet, P.; et al. Nanomole-scale high-throughput chemistry for the synthesis of complex molecules. *Science* **2015**, *347*, 49−53.

(50) Krska, S. W.; DiRocco, D. A.; Dreher, S. D.; Shevlin, M. The Evolution of Chemical High-Throughput Experimentation To Address Challenging Problems in Pharmaceutical Synthesis. *Acc. Chem. Res.* **2017**, *50*, 2976−2985.

(51) Mennen, S. M.; Alhambra, C. C.; Allen, C. L.; Barberis, M.; Berritt, S.; Brandt, T. A.; Campbell, A. D.; Castañón, J.; Cherney, A. H.; Christensen, M.; et al. The Evolution of High-Throughput Experimentation in Pharmaceutical Development and Perspectives on the Future. *Org. Process Res. Dev.* **2019**, *23*, 1213−1242.

(52) DiRocco, D. A.; Dykstra, K.; KrsKa, S.; Vachal, P.; Conway, D. V.; Tudge, M. Late-Stage Functionalizattion of Biologically Active Heterocycles Through Photoredox Catalysis. *Angew. Chem., Int. Ed.* **2014**, *53*, 4802−4806.

(53) Poznik, M.; König, B. Fast colorimetric screening for visible light photocatalytic oxidation and reduction reactions. *React. Chem. Eng.* **2016**, *1*, 494−500.

(54) Yayla, H. G.; Peng, F.; Mangion, I. K.; McLaughlin, M.; Campeau, L.-C.; Davies, I. W.; DiRocco, D. A.; Knowles, R. R. Discovery and mechanistic study of a photocatalytic indoline dehydrogenation for the synthesis of elbasir. *Chem. Sci.* **2016**, *7*, 2066−2073.

(55) ElMarrouni, A.; Ritts, C. B.; Balsells, J. Silyl-mediated photoredox-catalyzed Giese reaction: addition of non-activated alkyl bromides. *Chem. Sci.* **2018**, *9*, 6639−6646.

(56) Sun, A. C.; Steyer, D. J.; Allen, A. R.; Payne, E. M.; Kennedy, R. T.; Stephenson, C. R. J. A droplet microfluidic platform for high-throughput photochemical reaction discovery. *Nat. Commun.* **2020**, *11*, 6202−6207.

(57) Su, Y.; Straathof, N. J. W.; Hessel, V.; Noël, T. Photochemical Transformations Accelerated in Continuous-Flow Reactors: Basic Concepts and Applications. *Chem. - Eur. J.* **2014**, *20*, 10562−10589.

(58) Alfano, O. M.; Cassano, A. E.; Marugán, J.; van Grieken, R. Fundamentals of Radiation Transport in Absorbing Scattering Media. *Photocatalysis: Fundamentals and perspectives* **2016**, 349−366.

(59) Under conditions relevant to photoredox catalysis, the absorption coefficient can generally be simply described through the approximations of the Beer−Lambert law, while G_v, the spectral incident radiation, is a function of the spectral specific intensity, or the density of photons arriving at a point within the reaction for a given frequency per unit time, as integrated over all possible directions of photon propagation: Cassano, A. E.; Martín, C. A.; Brandi, R. J.; Alfano, O. M. Photoreactor Analysis and Design: Fundamentals and Applications. *Ind. Eng. Chem. Res.* **1995**, *34*, 2155−2201.

(60) The photon flux should be the same in both high-throughput experimentation and continuous systems. To ensure this, an actinometry study by ferrioxalate photon degradation was carried out for each system. Handling of the ferrioxalate was performed with extreme care to avoid ambient light exposure. Corcoran, E. B.; McMullen, J. P.; Lévesque, F.; Wismer, M. K.; Naber, J. R. Photon Equivalents as a Parameter for Scaling Photoredox Reactions in Flow: Translation of Photocatalytic C−N Cross-Coupling from Lab Scale to Multikilogram Scale. *Angew. Chem., Int. Ed.* **2020**, *59*, 11964−11968.

(61) We have tested commercial parallel systems, and they thus far have been unsuccessful in regard to either the efficiency of the reaction or any translation to flow systems (see Supporting Information).

(62) Zuo, Z.; Ahneman, D. T.; Chu, L.; Terrett, J. A.; Doyle, A. G.; MacMillan, D. W. C. Merging Photoredox with Nickel Catalysis: Coupling of α-Carboxyl sp3-Carbons with Aryl Halides. *Science* **2014**, *345*, 437−440.

(63) Wegner, J.; Ceylan, S.; Kirschning, A. Ten key issues in modern flow chemistry. *Chem. Commun.* **2011**, *47*, 4583−4592.

(64) Beatty, J. W.; Douglas, J. J.; Cole, K. P.; Stephenson, C. R. J. A scalable and operationally simple radical trifluoromethylation. *Nat. Commun.* **2015**, *6*, 7919.

(65) Johnston, C. P.; Smith, R. T.; Allmendinger, S.; MacMillan, D. W. C. Metallaphotoredox-catalysed sp3-sp3 cross-coupling of carboxylic acids with alkyl halides. *Nature* **2016**, *536*, 322−325.

(66) Liang, Y.; Zhang, X.; MacMillan, D. W. C. Decarboxylative sp3 C−N coupling via dual copper and photoredox catalysis. *Nature* **2018**, *559*, 83−88.

(67) Zhang, P.; Le, C.; MacMillan, D. W. C. Silyl Radical Activation of Alkyl Halides in Metallaphotoredox Catalysis: A Unique Pathway for Cross-Electrophile Coupling. *J. Am. Chem. Soc.* **2016**, *138*, 8084−8087.

(68) Harper, K. C.; Moschetta, E. G.; Bordawekar, S. V.; Wittenberger, S. J. A Laser Driven Flow Chemistry Platform for Scaling Photochemical Reactions with Visible Light. *ACS Cent. Sci.* **2019**, *5*, 109−115.

(69) Pomberger, A.; Mo, Y.; Nandiwale, K. Y.; Schultz, V. L.; Duvadie, R.; Robinson, R. I.; Altinoglu, E. I.; Jensen, K. F. A Continuous Stirred-Tank Reactor (CSTR) Cascade for Handling Solid-Containing Photochemical Reactions. *Org. Process Res. Dev.* **2019**, *23*, 2699−2706.

(70) Ravetz, B. D.; Tay, N. E. S.; Joe, C. L.; Sezen-Edmonds, M.; Schmidt, M. A.; Tan, Y.; Janey, J. M.; Eastgate, M. D.; Rovis, T. Development of a Platform for Near-Infrared Photoredox Catalysis. *ACS Cent. Sci.* **2020**, *6*, 2053−2059.

(71) Terrett, J. A.; Cuthbertson, J. D.; Shurtleff, V. W.; MacMillan, D. W. C. Switching on elusive organometallic mechanisms with photoredox catalysis. *Nature* **2015**, *524*, 330−334.